PHYSICAL REVIEW B **83**, 014401 (2011)

Robust ferroelectric state in multiferroic $Mn_{1-x}Zn_xWO_4$

R. P. Chaudhury,[1] F. Ye,[2] J. A. Fernandez-Baca,[2,3] B. Lorenz,[1] Y. Q. Wang,[1] Y. Y. Sun,[1] H. A. Mook,[2] and C. W. Chu[1,4]

[1]*Texas Center for Superconductivity and Department of Physics, University of Houston, Houston, Texas 77204-5002, USA*

[2]*Neutron Scattering Science Division, Oak Ridge National Laboratory, Oak Ridge, Tennessee 37831-6393, USA*

[3]*Department of Physics and Astronomy, University of Tennessee, Knoxville, Tennessee 37996-1200, USA*

[4]*Lawrence Berkeley National Laboratory, 1 Cyclotron Road, Berkeley, California 94720, USA*

(Received 29 October 2010; revised manuscript received 7 December 2010; published 10 January 2011)

We report on the remarkably robust ferroelectric state in the multiferroic compound $Mn_{1-x}Zn_xWO_4$. Substitution of the magnetic Mn^{2+} with nonmagnetic Zn^{2+} reduces the magnetic exchange and provides control of the various magnetic and multiferroic states of $MnWO_4$. Only 5% of Zn substitution results in complete suppression of the frustrated collinear (paraelectric) low-temperature phase. The helical magnetic and ferroelectric phase develops as the ground state. The multiferroic state is stable up to a high level of substitution of more than 50%. The magnetic, thermodynamic, and dielectric properties, as well as the ferroelectric polarization of single crystals of $Mn_{1-x}Zn_xWO_4$, are studied for different substitutions up to $x = 0.5$. The magnetic phases have been identified in single-crystal neutron-scattering experiments. The ferroelectric polarization scales with the neutron intensity of the incommensurate peak of the helical phase.

DOI: 10.1103/PhysRevB.83.014401 PACS number(s): 75.30.Kz, 75.50.Ee, 77.80.−e

I. INTRODUCTION

Multiferroic materials have received increasing attention in recent years because of the coexistence and mutual interaction of magnetic and ferroelectric orders and their coupling to external magnetic and electric fields.[1–3] Improper ferroelectricity can be induced by certain kinds of inversion symmetry-breaking magnetic order if the magnetic moments are strongly coupled to the lattice, causing the ionic displacements with a macroscopic electrical polarization. The transverse helical magnetic structure was shown to be compatible by symmetry with a ferroelectric polarization arising from a third-order coupling term of the ferroelectric and magnetic-order parameters in the Ginzburg-Landau thermodynamic potential.[4,5] Helical (noncollinear) magnetic structures have in fact been found in various multiferroics, for example, in $TbMnO_3$,[4] $Ni_3V_2O_8$,[6] and $MnWO_4$.[7,8] Different microscopic models have been proposed recently to describe the phase complexity and ferroelectricity in multiferroic manganites.[9–12]

The noncollinear magnetic order observed in these compounds is a consequence of magnetic frustration due to geometric constraints or competing exchange interactions, resulting in a close competition of different magnetic structures that are nearly equal in energy. Most multiferroic materials are therefore extremely sensitive to small perturbations. Magnetic fields may stabilize or destroy the multiferroic state or result in the rotation of the ferroelectric polarization by 90° or even by 180°.[7,13–15] Similarly, the application of external pressure[16–19] as well as chemical substitutions[20–23] are viable tools to change and tune the multiferroic properties of different compounds.

$MnWO_4$ is also known as the mineral hübnerite. The crystallographic structure of the compound is monoclinic (space group: $P\ 2/c$). Three magnetic phase transitions at $T_N = 13.5$ K, $T_C = 12.6$ K, and $T_L = 7.8$ K separate different collinear and noncollinear magnetic phases.[24] The AF3 phase ($T_C < T < T_N$) shows a sinusoidal spin order given by the incommensurate (IC) vector $\vec{q}_3 = (-0.214, 1/2, 0.457)$. The collinear Mn spins are confined to the *a*-*c* plane, forming an angle of about 34° with the *a* axis. Below T_C the spins tilt out of plane and form a helical, noncollinear structure, breaking the spatial inversion symmetry (AF2 phase). The modulation vector of the spin order does not change at T_C, $\vec{q}_2 = \vec{q}_3$. The helical phase becomes unstable at T_L, and the low-temperature AF1 phase (ground state) is characterized by a frustrated $\uparrow\uparrow\downarrow\downarrow$ spin structure with a commensurate (CM) modulation vector $\vec{q}_1 = (-1/4, 1/2, 1/2)$. Among the three magnetic phases, only the helical AF2 phase is ferroelectric. The details of the magnetic structures have been revealed in neutron-scattering experiments.[24,25] The complex phase diagram of $MnWO_4$ and the multiferroic properties have been described extensively through magnetic, dielectric, and thermodynamic measurements.[7,8,26–29] Novel physical phenomena, such as the coupling of ferroelectric with magnetic domains[30] or control of the magnetic domain chirality by electric fields,[31] have been reported.

Tuning of the magnetic exchange interactions and, consequently, the multiferroic properties by partial substitution of manganese by other transition metals, for example, iron or cobalt, was achieved recently.[32–36] The magnetic phases and the multiferroic properties are extremely sensitive to small amounts of Fe substitution.[20,21,37] Some of the observed effects of transition-metal substitution can be qualitatively described by simple Heisenberg models with competing interactions and uniaxial anisotropy.[20,38] However, a more quantitative and microscopic understanding of the complex magnetic interactions and the effects of Fe or Co substitution is challenging, because Fe as well as Co carry their own magnetic moments, and their exchange interactions with the Mn spins and their anisotropy parameters are not known. To overcome some of these problems and to simplify the physics of magnetic exchange in substituted $MnWO_4$, we decided to replace the Mn^{2+} by nonmagnetic *d* metals such as Zn^{2+}. We therefore synthesized single crystals of $Mn_{1-x}Zn_xWO_4$ with *x* between 0 and 0.5 and investigated their magnetic, thermodynamic, and multiferroic properties.

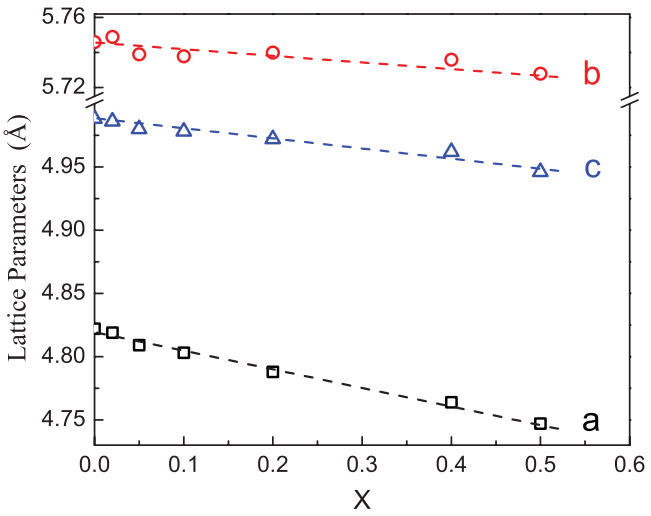

FIG. 1. (Color online) Lattice constants a, b, and c of $Mn_{1-x}Zn_xWO_4$ as a function of x.

II. EXPERIMENTAL

The crystals were grown from a polycrystalline feed rod employing a floating-zone optical furnace. The x-ray characterization shows that the a and c axes significantly decrease with the Zn substitution (Fig. 1), whereas the b axis shows only a minor decrease within the resolution of the measurements. The smooth change of a, b, and c indicates that a solid solution of $MnWO_4$ and $ZnWO_4$ has formed. Small pieces were cut from the crystals and oriented using Laue single-crystal x-ray techniques. The size and shape of the crystals were carefully chosen to fit the demands of the different experiments. The susceptibility was measured in a 5-T magnetic property measurement system (MPMS, Quantum Design). The ferroelectric polarization of the multiferroic phase was measured by integrating the pyroelectric current upon heating the sample in zero electric field at a speed of 1 K/min. Before the pyroelectric measurement the sample was cooled in an electric bias field of 3 kV/cm to align the ferroelectric domains. The heat capacity was measured in a physical property measurement system (PPMS, Quantum Design). The elastic neutron-scattering measurements were performed at the HB1A and HB1 three-axis spectrometers at the High Flux Isotope Reactor at the Oak Ridge National Laboratory. The crystals were aligned in the scattering plane defined by the two orthogonal wave vectors $(1,0,-2)$ and $(0,1,0)$, in which the magnetic Bragg peaks and other structural peaks can be surveyed. The incident neutron energy was fixed at 14.7 meV using pyrolytic graphite crystals as monochromator, analyzer, and filter.

III. RESULTS AND DISCUSSION

The b-axis magnetic susceptibility at high temperatures ($T > 50$ K) follows the Curie-Weiss law, as shown in Fig. 2. From the inverse susceptibility the effective magnetic moment μ_{eff} per formula unit ($Mn_{1-x}Zn_xWO_4$), as well as the Curie-Weiss temperature, Θ_W values can be extracted and are displayed in the inset of Fig. 2. As expected for dominantly antiferromagnetic coupling, Θ_W is negative and

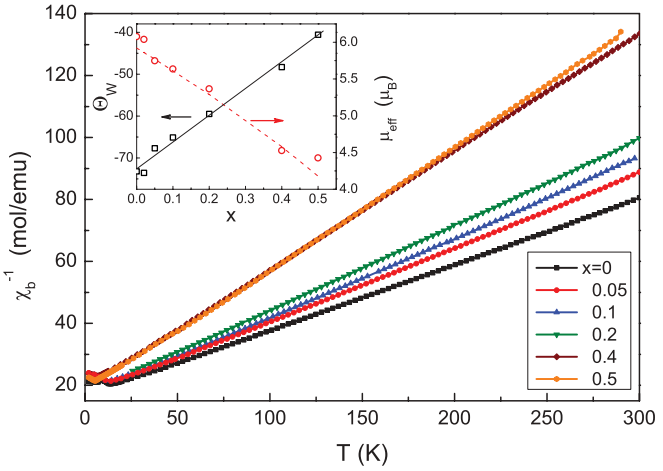

FIG. 2. (Color online) Inverse magnetic susceptibility of $Mn_{1-x}Zn_xWO_4$. The inset shows the x dependence of the estimated effective magnetic moment μ_{eff} and the Curie-Weiss temperature θ_W. The dashed line is the expected μ_{eff} for a Mn spin of $S = 5/2$. The black (solid) line is a linear fit to the data of Θ_W.

its magnitude decreases with Zn substitution, indicating the weakening of the magnetic coupling between the Mn spins. The effective magnetic moment also decreases with x, since the Zn substitution continuously dilutes the system of Mn spins. The expected values for μ_{eff}, assuming localized spins of the Mn^{2+} ions with $S = 5/2$, are shown by the dashed line in the inset of Fig. 2. The experimentally determined values for μ_{eff} are in very good agreement with the calculated values, confirming the conclusion that the Zn^{2+} substitutes for the Mn^{2+} at levels up to the maximum of this work, 50%. This is further confirmed by inductively coupled plasma mass spectrometry, testing the elemental composition at ten different spots of a single crystal with nominally 50% Zn doping. The average Zn concentration was determined as 0.49 ± 0.03, close to the nominal composition.

The b-axis magnetic susceptibility at low temperatures clearly reveals the magnetic phase transitions at T_N and T_L, as shown in Fig. 3 (different curves are vertically offset for

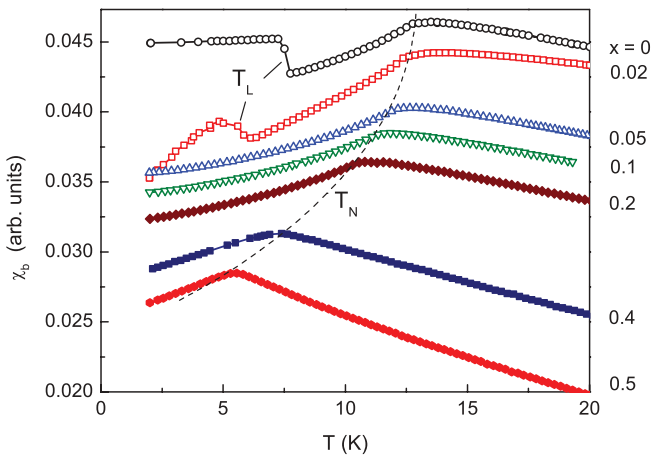

FIG. 3. (Color online) Low-temperature magnetic susceptibility χ_b of $Mn_{1-x}Zn_xWO_4$. Different curves are vertically offset for enhanced clarity.

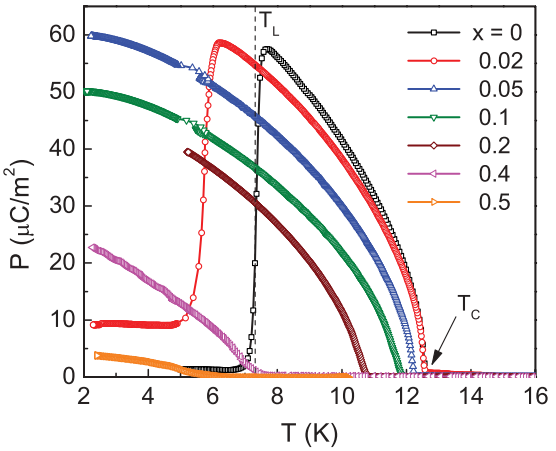

FIG. 4. (Color online) Ferroelectric polarization of $Mn_{1-x}Zn_xWO_4$ in zero magnetic field. T_N and T_L are labeled for the $x = 0$ data.

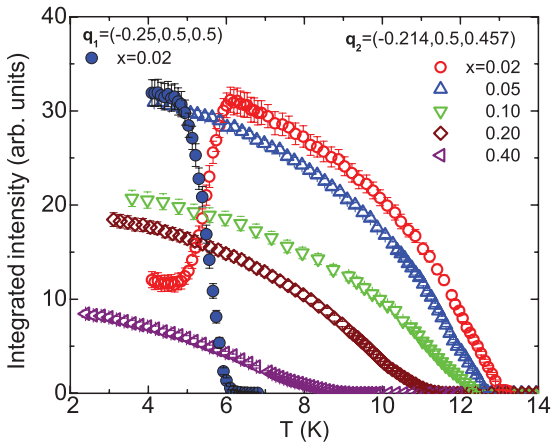

FIG. 5. (Color online) Neutron-scattering intensities of the incommensurate [open symbols, $q_2 = (-0.214,1/2,0.457)$] and commensurate [filled symbols, $q_1 = (-0.25,0.5,0.5)$] peaks of $Mn_{1-x}Zn_xWO_4$.

better clarity). The transition into the AF3 phase is defined by the maximum of $\chi_b(T)$, as indicated by the dashed line labeled T_N. With the lock-in transition into the AF1 phase, χ_b shows a sharp increase at T_L that is quickly shifted to lower temperatures with increasing x and is completely missing for $x \geqslant 0.05$. Only 5% of Zn substitution is sufficient to suppress the collinear AF1 phase and to stabilize the multiferrroic ferroelectric phase as the ground state. The effect of Zn substitution is opposite of the results of Fe substitution,[21] where the multiferroic AF2 phase was suppressed and the low-T AF1 phase was stabilized with increasing Fe content. A similar stabilization of the AF2 phase was reported for Co-substituted $MnWO_4$ powder samples,[36] although the magnetic phases of $Mn_{1-x}Co_xWO_4$ are far more complex, and several coexisting commensurate and incommensurate phases have been observed in single crystals at higher Co doping.[39]

The main feature of the multiferroic phase is the existence of a spontaneous ferroelectric polarization that is oriented along the b axis. Figure 4 shows $P_b(T)$ of $Mn_{1-x}Zn_xWO_4$ for x between 0 and 0.5, as measured by the pyroelectric current method. In perfect agreement with the magnetic data, the ferroelectric phase extends to the lowest temperature for x values equal to or above 5%. The multiferroic phase becomes the ground state and it exists even at substitution levels as high as 50%, while the onset temperature T_C is reduced with increasing x. It is interesting that the 2% substitution does decrease T_L rapidly, but there remains a finite polarization in the low-temperature state, indicating the coexistence of the AF1 and AF2 phases. Similar phase coexistence has also been observed in recent single-crystal neutron-scattering experiments on $Mn_{1-x}Fe_xWO_4$[37,40] and $Mn_{0.85}Co_{0.15}WO_4$.[39] At higher substitution levels the ferroelectric polarization increases continuously with decreasing temperature. The polarization data of Fig. 4 prove that unlike the Fe-substituted system $Mn_{1-x}Fe_xWO_4$, the substitution of the nonmagnetic Zn ion favors the multiferroic ferroelectric state that becomes the ground state for $x \geqslant 0.05$.

To identify the magnetic orders and their development with increasing Zn substitution, neutron-scattering experiments have been conducted. The temperature dependence of the integrated magnetic peak intensities in doped $Mn_{1-x}Zn_xWO_4$ is displayed in Fig. 5. The measurements were performed near the characteristic magnetic wave vector $\vec{q}_2 = (-0.214,1/2,0.457)$ for the AF2 phase associated with the ferroelectric behavior. At the lowest Zn concentration $x = 0.02$, the peak intensity first increases upon cooling below 13 K, is significantly suppressed below 6 K, but remains finite at lower temperature. Such behavior is accompanied by the sudden appearance of the commensurate magnetic order with $\vec{q}_1 = (-0.25,0.5,0.5)$ below $T_L = 6$ K (solid circles in Fig. 5). For higher Zn-doping systems, only incommensurate magnetic orders exist at all temperatures, and the thermal evolution of the integrated intensity closely tracks the polarization measurement, which shows the intimate connection between the spiral order and the ferroelectricity.

At the high-temperature side the onset of magnetic order (AF3 phase) is clearly visible in the sudden increase of the neutron intensities at T_N. The transition from the sinusoidal AF3 phase to the helical AF2 phase at T_C is more difficult to detect because both phases have the same magnetic modulation vector. A small change of slope and an anomaly in the width of the magnetic scattering peak is associated with the AF3→AF2 transition. The derived critical temperatures, T_N and T_C, are included in the phase diagram of Fig. 6 (triangles).

Similarly, the two transitions at T_N and T_C are also difficult to distinguish in the magnetization data of Fig. 3. The heat capacity $C_p(T)$, however, shows two well-defined sharp anomalies at the two phase transitions, a sharp rise and peak at T_N, and a second peak at T_C. We measured the heat capacity for all samples as shown in Fig. 7. Both transitions are well resolved, although the width of the transitions slightly increases with x. For the undoped $MnWO_4$ ($x = 0$), the sharp peak at 7.8 K indicates the first-order phase transition into the AF1 phase. The $T - x$ phase diagram is constructed from heat capacity, magnetization, and polarization measurements (Fig. 6). The commensurate AF1 phase is completely suppressed for $x \geqslant 0.05$. The finite value of the low-temperature

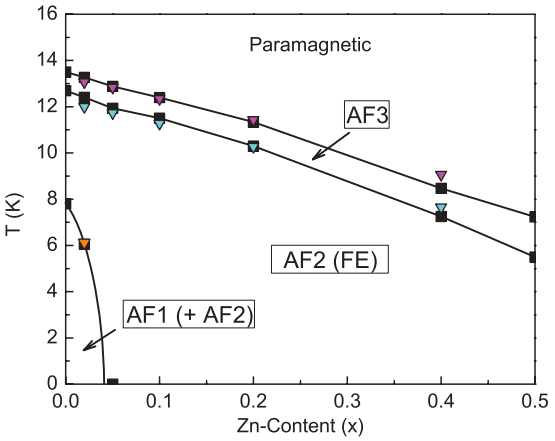

FIG. 6. (Color online) Multiferroic phase diagram of $Mn_{1-x}Zn_xWO_4$. The low-temperature phase below $x = 0.05$ is a mixed phase, AF1 + AF2. Squares denote data from magnetic, heat capacity, and polarization measurements. Triangles are data from neutron scattering.

polarization for $x = 0.02$ reveals the coexistence of AF1 and AF2 below T_L, as confirmed by the neutron-scattering experiments (Fig. 5).

The two phases (AF1 + AF2) coexisting for $x \leqslant 0.05$ at low T can be tuned by external magnetic fields, and the degeneracy is completely lifted above a critical field. This is best demonstrated in measuring the ferroelectric polarization of $Mn_{0.98}Zn_{0.02}WO_4$ in external magnetic fields with different orientations (Fig. 8). With the field directed along the spin easy axis (a-c plane, Fig. 8a), the low-T polarization ($T < T_L$) rapidly increases and for $H \geqslant 2$ T, the small drop of P_b at T_L is gone. The magnetic field has completely suppressed the AF1 phase and the multiferroic AF2 phase extends entirely to zero temperature. However, with the field applied along the b axis (Fig. 8b), the low-T polarization decreases and reaches zero

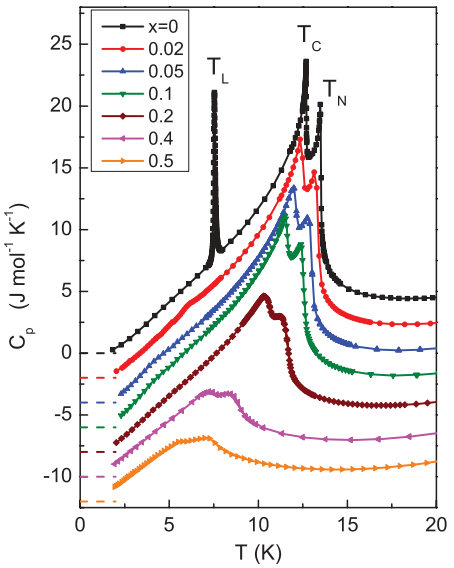

FIG. 7. (Color online) Heat capacity C_p/T of $Mn_{1-x}Zn_xWO_4$ in zero magnetic field. Different curves are vertically offset by two units (zero is defined by the dashed line for each curve).

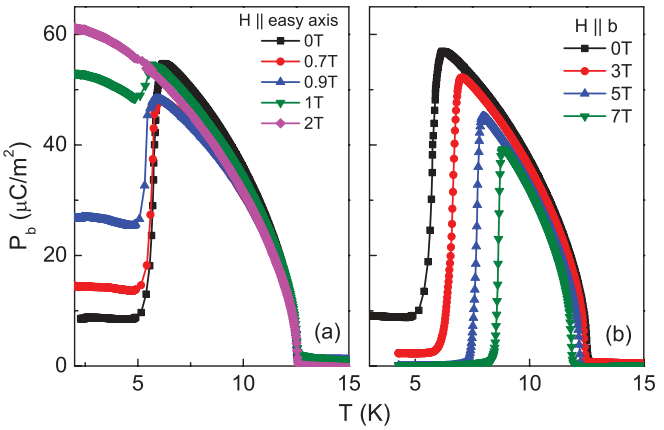

FIG. 8. (Color online) Magnetic field effect on the polarization of $Mn_{0.98}Zn_{0.02}WO_4$. The phase coexistence at low T is lifted in external fields.

above 3 T. The low-temperature phase and the ground state are now the AF1 phase and the degeneracy of both phases is removed. The lock-in transition temperature increases with H_b from 5.7 K (zero field) to 8.7 K at 7 T.

IV. SUMMARY AND CONCLUSIONS

We have shown that the multiferroic AF2 phase in $Mn_{1-x}Zn_xWO_4$ is remarkably stable with respect to the dilution of the magnetic exchange couplings induced by the substitution of nonmagnetic Zn ions. At low substitution levels and low temperatures a coexistence of two phases, the paraelectric AF1 phase and the ferroelectric AF2 phase, is shown. External magnetic fields do resolve the degeneracy of the two phases. Depending on the orientation of the magnetic field, either one of the coexisting states may become the ground state.

The rapid suppression of the collinear AF1 phase by less than 5% Zn doping and the survival of the sinusoidal AF3 and helical AF2 phases with up to 50% substitution is unique and distinguishes the multiferroic $MnWO_4$ from other multiferroics with a similar phase sequence, for example, $Ni_3V_2O_8$.[6] In the latter compound it was shown that the magnetic and multiferroic phases are strongly suppressed with the substitution of the magnetic Ni by nonmagnetic Zn, consistent with a two-dimensional spin system.[41] In $MnWO_4$, however, the relatively small effect of the dilution of the system of Mn spins through Zn doping on the AF3 and AF2 critical temperatures indicates a three-dimensional character of the basic magnetic exchange interactions. The microscopic exchange interactions can be revealed through inelastic neutron scattering (INS) experiments probing the magnetic excitations. By comparing the magnon spectra with standard models the most relevant exchange parameters can be extracted. According to recent INS experiments on $MnWO_4$, short-range (nearest and next-nearest neighbors) exchange interactions are not sufficient to explain the magnetic excitation spectrum, but up to 11 different exchange pathways have to be involved to fit the data.[42,43] The higher order exchange coupling constants involved in the magnetic correlations prove the three-dimensional character of the magnetic fluctuations.

In three dimensions the percolation threshold for site dilution is much lower than for two-dimensional systems, explaining the robustness of the magnetic orders (AF3 and AF2) in Zn-doped $MnWO_4$.

The low-temperature AF1 phase, however, is in strong competition with the helical AF2 state. A simple mean-field model calculation has shown that the phase boundary between AF1 and AF2 as a function of competing exchange coupling and anisotropy constants can be very steep and extremely sensitive with respect to small perturbations.[20,44] The frustration of different magnetic states results in a deviation from the mean-field result for suppression of the critical temperature as a function of doping level in a diluted magnetic system and the strong suppression of the AF1 phase as observed in $Mn_{1-x}Zn_xWO_4$.

Note added. After submission of this manuscript the authors became aware of a related investigation of polycrystalline $MnWO_4$ doped with Mg and Zn up to 30%.[45] The conclusions derived from the magnetization and dielectric constant data are consistent with the phase diagram of Fig. 7.

ACKNOWLEDGMENTS

This work is supported in part by the T.L.L. Temple Foundation, the J. J. and R. Moores Endowment, and the State of Texas through TCSUH and at LBNL through the US DOE, Contract No. DE-AC03-76SF00098. The research at Oak Ridge National Laboratory's High Flux Isotope Reactor was sponsored by the Scientific User Facilities, Office of Basic Energy Sciences, US Department of Energy.

[1] M. Fiebig, J. Phys. D: Appl. Phys. **38**, R123 (2005).
[2] N. A. Spaldin and M. Fiebig, Science **309**, 391 (2005).
[3] Y. Tokura, J. Magn. Magn. Mater. **310**, 1145 (2007).
[4] M. Kenzelmann, A. B. Harris, S. Jonas, C. Broholm, J. Schefer, S. B. Kim, C. L. Zhang, S.-W. Cheong, O. P. Vajk, and J. W. Lynn, Phys. Rev. Lett. **95**, 087206 (2005).
[5] M. Mostovoy, Phys. Rev. Lett. **96**, 067601 (2006).
[6] G. Lawes, A. B. Harris, T. Kimura, N. Rogado, R. J. Cava, A. Aharony, O. Entin-Wohlman, T. Yildrim, M. Kenzelmann, C. Broholm, and A. P. Ramirez, Phys. Rev. Lett. **95**, 087205 (2005).
[7] K. Taniguchi, N. Abe, T. Takenobu, Y. Iwasa, and T. Arima, Phys. Rev. Lett. **97**, 097203 (2006).
[8] O. Heyer, N. Hollmann, I. Klassen, S. Jodlauk, L. Bohaty, P. Becker, J. A. Mydosh, T. Lorenz, and D. Khomskii, J. Phys. Condens. Matter **18**, L471 (2006).
[9] H. Katsura, N. Nagaosa, and A. V. Balatsky, Phys. Rev. Lett. **95**, 057205 (2005).
[10] I. A. Sergienko and E. Dagotto, Phys. Rev. B **73**, 094434 (2006).
[11] I. A. Sergienko, C. Sen, and E. Dagotto, Phys. Rev. Lett. **97**, 227204 (2006).
[12] M. Mochizuki, N. Furukawa, and N. Nagaosa, Phys. Rev. Lett. **105**, 037205 (2010).
[13] D. Higashiyama, S. Miyasaka, N. Kida, T. Arima, and Y. Tokura, Phys. Rev. B **70**, 174405 (2004).
[14] N. Hur, S. Park, P. A. Sharma, S. Guha, and S.-W. Cheong, Phys. Rev. Lett. **93**, 107207 (2004).
[15] S. Seki, Y. Yamasaki, M. Soda, M. Matsuura, K. Hirota, and Y. Tokura, Phys. Rev. Lett. **100**, 127201 (2008).
[16] C. R. dela Cruz, B. Lorenz, Y. Y. Sun, Y. Wang, S. Park, S.-W. Cheong, M. M. Gospodinov, and C. W. Chu, Phys. Rev. B **76**, 174106 (2007).
[17] C. R. dela Cruz, B. Lorenz, and C. W. Chu, Physica B **403**, 1331 (2008).
[18] R. P. Chaudhury, F. Yen, C. R. dela Cruz, B. Lorenz, Y. Q. Wang, Y. Y. Sun, and C. W. Chu, Phys. Rev. B **75**, 012407 (2007).
[19] R. P. Chaudhury, C. R. dela Cruz, B. Lorenz, Y. Sun, C. W. Chu, S. Park, and S.-W. Cheong, Phys. Rev. B **77**, 220104(R) (2008).
[20] R. P. Chaudhury, B. Lorenz, Y. Q. Wang, Y. Y. Sun, and C. W. Chu, Phys. Rev. B **77**, 104406 (2008).
[21] R. P. Chaudhury, B. Lorenz, Y.-Q. Wang, Y. Y. Sun, and C. W. Chu, New J. Phys. **11**, 033036 (2009).
[22] S. Seki, Y. Yamasaki, Y. Shiomi, S. Iguchi, Y. Onose, and Y. Tokura, Phys. Rev. B **75**, 100403(R) (2007).
[23] S. Kanetsuki, S. Mitsuda, T. Nakajima, D. Anazawa, H. A. Katori, and K. Prokes, J. Phys. Condens. Matter **19**, 145244 (2007).
[24] G. Lautenschläger, H. Weitzel, T. Vogt, R. Hock, A. Bohm, M. Bonnet, and H. Fuess, Phys. Rev. B **48**, 6087 (1993).
[25] H. Sagayama, K. Taniguchi, N. Abe, T. H. Arima, M. Soda, M. Matsuura, and K. Hirota, Phys. Rev. B **77**, 220407(R) (2008).
[26] H. Ehrenberg, H. Weitzel, C. Heidy, H. Fuess, G. Wltschek, T. Kroener, J. van Tol, and M. Bonner, J. Phys. Condens. Matter **9**, 3189 (1997).
[27] A. H. Arkenbout, T. T. M. Palstra, T. Siegrist, and T. Kimura, Phys. Rev. B **74**, 184431 (2006).
[28] K. Taniguchi, N. Abe, H. Sagayama, S. Otani, T. Takenobu, Y. Iwasa, and T. Arima, Phys. Rev. B **77**, 064408 (2008).
[29] R. P. Chaudhury, F. Yen, C. R. dela Cruz, B. Lorenz, Y. Q. Wang, Y. Y. Sun, and C. W. Chu, Physica B **403**, 1428 (2008).
[30] D. Meier, M. Maringer, T. Lottermoser, P. Becker, L. Bohaty, and M. Fiebig, Phys. Rev. Lett. **102**, 107202 (2009).
[31] T. Finger, D. Senff, K. Schmalzl, W. Schmidt, L. P. Regnault, P. Becker, L. Bohaty, and M. Braden, Phys. Rev. B **81**, 054430 (2010).
[32] H. A. Obermayer, H. Dachs, and H. Schröcke, Solid State Commun. **12**, 779 (1973).
[33] C. Klein and R. Geller, J. Phys. **35**, C6-589 (1974).
[34] E. Garcia-Matres, N. Stüßer, M. Hofmann, and M. Reehuis, Eur. Phys. J. B **32**, 35 (2003).
[35] Y. Ding, N. Stüßer, M. Reehuis, M. Hofmann, G. Ehlers, D. Günther, M. Meißner, S. Welzel, M. Wilhelm, M. Steiner, and F. Kubanek, Physica B **276–278**, 596 (2000).
[36] Y.-S. Song, J.-H. Chung, J. M. S. Park, and Y.-N. Choi, Phys. Rev. B **79**, 224415 (2009).

[37]F. Ye, Y. Ren, J. A. Fernandez-Baca, H. A. Mook, J. W. Lynn, R. P. Chaudhury, Y.-Q. Wang, B. Lorenz, and C. W. Chu, Phys. Rev. B **78**, 193101 (2008).

[38]G. Lawes, M. Kenzelmann, N. Rogado, K. H. Kim, G. A. Jorge, R. J. Cava, A. Aharony, O. Entin-Wohlman, A. B. Harris, T. Yildirim, Q. Z. Huang, S. Park, C. Broholm, and A. P. Ramirez, Phys. Rev. Lett. **93**, 247201 (2004).

[39]R. P. Chaudhury, F. Ye, J. A. Fernandez-Baca, Y. Q. Wang, Y. Y. Sun, B. Lorenz, H. A. Mook, and C. W. Chu, Phys. Rev. B **82**, 184422 (2010).

[40]R. P. Chaudhury, B. Lorenz, Y. Q. Wang, Y. Y. Sun, C. W. Chu, F. Ye, J. Fernandez-Baca, H. Mook, and J. Lynn, J. Appl. Phys. **105**, 07D913 (2009).

[41]P. Kharel, A. Kumarasiri, A. Dixit, N. Rogado, R. J. Cava, and G. Lawes, Philos. Mag. **89**, 1923 (2009).

[42]H. Ehrenberg, H. Weitzel, H. Fuess, and B. Hennion, J. Phys. Condens. Matter **11**, 2649 (1999).

[43]F. Ye, R. S. Fishman, J. A. Fernandez-Baca, A. A. Podlesnyak, G. Ehlers, H. A. Mook, Y.-Q. Wang, B. Lorenz, and C. W. Chu (submitted for publication).

[44]M. Kenzelmann, A. B. Harris, A. Aharony, O. Entin-Wohlman, T. Yildirim, Q. Huang, S. Park, G. Lawes, C. Broholm, N. Rogado, R. J. Cava, K. H. Kim, G. Jorge, and A. P. Ramirez, Phys. Rev. B **74**, 014429 (2006).

[45]L. Meddar, M. Josse, P. Deniard, C. La, G. André, F. Damay, V. Petricek, S. Jobic, M.-H. Whangbo, M. Maglione, and C. Payen, Chem. Mater. **21**, 5203 (2009).